JOURNAL OF MAGNETIC RESONANCE **126,** 103–109 (1997)
ARTICLE NO. MN971148

In Vitro Validation of Rapid MR Measurement of Wave Velocity

Kenneth A. Kraft,* Panos P. Fatouros,* Frank D. Corwin,* and Ding-Yu Fei†

*Department of Radiology, P.O. Box 980072, and †Department of Biomedical Engineering, Virginia Commonwealth University, Richmond, Virginia 23298-0072

Received December 24, 1996; revised February 14, 1997

A one-dimensional time-of-flight MR sequence, having a total acquisition time of approximately 60 ms, has been employed to determine flow-wave propagation velocities for pulsatile flow in compliant latex tubes. The results were compared with those of two independent methods and were found to be in good agreement. An extension of the same MR method was used to test the validity of the "water-hammer" relationship as a means to assess pulse pressure. Very good agreement was found with direct manometric determinations of pulse pressure. © 1997 Academic Press

INTRODUCTION

The rate of propagation of the flow or pressure wave in arteries has long been recognized as a measure of vascular compliance, which is physiologically important for several reasons. Part of the energy of left ventricular contraction is stored as potential energy in the distention of the large elastic arteries. During diastole, elastic recoil helps to maintain forward flow, thus converting the pulsatile output of the heart into steady capillary flow (*1*). In addition, proper arterial compliance mitigates the potentially injurious effects of wave reflections, by delaying their arrival in the central vasculature until early diastole. By rapidly convecting pressure waves in both the forward and reverse directions, stiffer arteries hasten the arrival of reflections, which may return to the aorta during mid- to late systole, thereby elevating the central pulse pressure, attenuating forward blood flow, and augmenting left ventricular afterload (*2*). Increased central arterial stiffness is generally associated with aging, sedentary lifestyle, and certain vascular and systemic diseases.

Another hemodynamically significant parameter is the pulse pressure, which is defined as the difference between systolic and diastolic pressure. Because pulse pressure can vary between the central and peripheral arteries, conventional brachial arterial sphygmomanometry may not accurately reflect the pressure dynamics in the aorta. There is evidence that elevations in aortic pulse pressure can occur without causing changes in the conventional peripheral measurement (*3*). It follows, therefore, that effective therapeutic palliation of central pulse pressure may be undetectable by conventional means and underscores the need for a noninvasive measurement of central pulse pressure (*4*).

Noninvasive determinations of flow-wave velocities have previously been carried out using Doppler ultrasound (*5*), applanation tonometry (*6*), and MR methods (*7–10*). Most sequences based on the latter are designed to measure blood velocity at two or more spatial locations or along a selected arterial segment with sufficient temporal resolution to resolve the rapidly propagating flow wavefront. Clearly, methods which rely on interleaving of multiple incrementally gated data acquisitions are subject to errors introduced by timing irregularities. Most desirable are techniques which complete the measurement within a single systolic pulse. For any proposed method, *in vitro* assessment of its accuracy against an established standard should be carried out. With few exceptions (*11*), however, published reports to date have included no validation of MR wave velocity results against proven measurement methods.

The main purpose of this study is to evaluate, using well-characterized *in vitro* models, a two-slice projective MR sequence for rapid determination of flow-wave propagation velocities. The results obtained using compliant latex tube models of arterial segments are compared with direct determinations of pressure wavespeeds, as well as with theoretical wave velocities based on measured pressure-expansion curves for the same tubes. A second objective is to validate the accuracy of the so-called water-hammer equation (*12*) for predicting pulse pressure based on the MR-measurable parameters of wave velocity and peak flow velocity.

THEORY

The distensibility (D) of a vessel is defined (*13*) as the fractional change in cross-sectional area (A) per unit change in pressure (P), i.e.,

$$D = \frac{dA}{A\,dP}. \qquad [1]$$

The wave velocity, c, is related to distensibility via the expression

$$c = \sqrt{\frac{1}{\rho D}}, \qquad [2]$$

1090-7807/97 $25.00

where ρ is the fluid density. The wave velocity may also be directly assessed by determining the time delay between pressure or flow waveforms measured at two or more sites in a vessel, and dividing the temporal delay by the known separation distance. To avoid the potentially confounding effects of wave reflection on the measured waveforms, time delays are typically measured at early systole (e.g., at the base or ''foot'' of the systolic flow or pressure peaks). The *in vivo* range for c is 2–15 m/s, and normally far exceeds the blood velocity. However, the observed wave velocity will be influenced by any motion of the fluid itself and must therefore be corrected when flow is present. If, for example, in addition to the pulsatile flow, there exists a forward steady flow component, the measured wave velocity will be altered commensurately, such that the ''true'' wavespeed is taken to be (*1*)

$$c = c_{\text{obs}} - v_{\text{fluid}}, \qquad [3]$$

where c_{obs} is the wavespeed measured in the presence of flow, and v_{fluid} is the spatial average fluid velocity (the steady flow velocity in this case). By the same reasoning, if the reference points for determining the temporal delay are chosen within the acceleration phase of systole (instead of the ''foot''), Eq. [3] should likewise be employed to compensate for the (higher) fluid velocity extant at the instant of measurement.

The pulse pressure (ΔP) can be calculated using the water-hammer equation (*12*)

$$\Delta P = \rho v_{\text{pk}} c \qquad [4]$$

and is given as the product of the fluid density, the temporal peak (spatial average) fluid velocity, and the wave velocity. Although Eq. [4] provides a potentially useful means to access aortic pulse pressure noninvasively, little experimental evidence of its validity exists in the literature (*14*).

METHODS

All MR data were acquired using a Bruker ABX Biospec spectrometer (Bruker Instruments, Billerica, Massachusetts) interfaced to a 2.35 T, 40 cm bore superconducting magnet equipped with a 11.6 cm i.d. actively shielded gradient coil insert. A 76 mm i.d. quadrature radiofrequency coil of a birdcage design was used for both RF excitation and signal reception.

The flow apparatus was designed to permit fluid-bearing tubing to pass through the horizontal-bore MR magnet such that pulsatile volume flow and resting pressure could be controlled and monitored. The fluid circuit consisted of an elevated source tank, a pulsatile pump (Model D141, Liquid Metronics, Acton, Massachusetts), the test section within the magnet, and a small receiving tank. The elevation of the receiving tank was varied to adjust the quiescent pressure within the test section; its overflow was directed to a third (collecting) tank, with a recirculating pump to replenish the source tank and thereby complete the flow circuit. The fluid was an aqueous solution of dextran and nickel chloride, which mimicked blood in terms of its viscosity and MR relaxivity. Flow rates were monitored using an in-line ultrasonic flowmeter (Model T101, Transonic Systems, Ithaca, New York), which was placed between the pulsatile pump and the test section. The flow trace was displayed on a digital storage oscilloscope and was also directed to an adjustable trigger generator to create a TTL pulse used to initiate MR data acquisition. Relatively stiff vinyl tubing was used between the pulsatile pump and the magnet in order to avoid excessive damping of the pulsatile fluid impulse before it reached the compliant test tubing. Two test materials were used for the experiments described herein: $\frac{1}{2}$ inch i.d. (12.7 mm) latex (Penrose surgical drain tubing, wall thickness approximately 0.3 mm), and $\frac{3}{4}$ inch i.d. (19 mm) latex laboratory tubing having $\frac{1}{8}$ inch (3.2 mm) wall thickness. For convenience, these tubes may be henceforth distinguished as ''thin-wall'' and ''thick-wall,'' respectively. The thin-wall latex tubing was constrained from moving longitudinally during pulsatile flow experiments by lightly resting it on a strip of double-sided adhesive tape running the length of the supporting platform within the magnet. Pressure monitoring was accomplished by piercing the tubing with a short 23 G hypodermic needle attached to a transducer (Abbott Laboratories, Chicago, Illinois) and flushing with degassed water to eliminate air bubbles. The transducer output was directed to a calibrated dual-channel amplifier (Triton Technology, San Diego, California) and then displayed on the oscilloscope. For determining pressure wave propagation rates, two transducers positioned just outside either end of the RF coil were simultaneously monitored.

Direct distensibility measurements were performed by acquiring multiple high-resolution (100 μm in-plane) cross-sectional MR images of the latex tubes at a series of static pressures. All images of a series were rescaled identically and masked using a fixed minimum intensity threshold to exclude pixels outside the lumen. The remaining pixels were taken to represent the luminal area. A plot of luminal area versus pressure (Fig. 1) was then fitted with a polynomial function (PSI-Plot, Poly Software Intl., Salt Lake City, Utah). The distensibility (Eq. [1]) was evaluated as a function of intraluminal pressure by numerically differentiating the fitted curve equation and dividing by the corresponding luminal area at each pressure setting. After converting units from mm Hg to dyn/cm^2 (and assuming a fluid density of 1.0 g/cm^3), the predicted wavespeed (Eq. [2]) at each pressure level was taken as the square root of the inverse of the distensibility.

Dynamic MR measurements of wave velocities in the la-

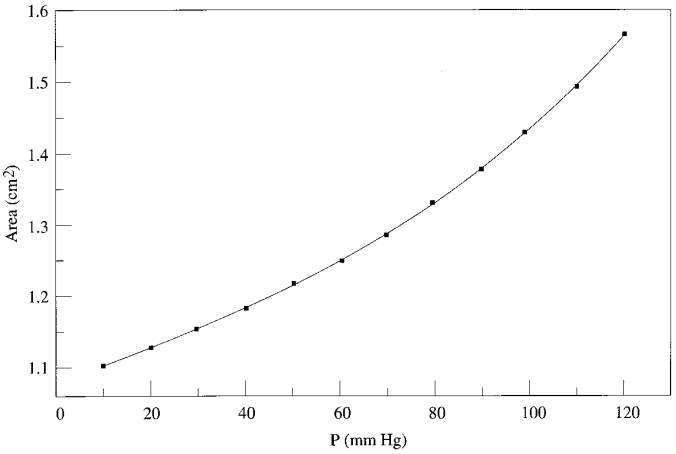

FIG. 1. The luminal area of the thin-wall (nominally $\frac{1}{2}$ inch i.d.) latex tubing (measured using cross-sectional MR imaging) as a function of the static pressure (measured manometrically).

tex tubes were also carried out using the high-speed projective time-of-flight sequence. A timing diagram of the sequence is presented in Fig. 2a, and a schematic illustration of its mode of action upon the sample is shown in Fig. 2b. By alternately pulsing and acquiring data from two spatially separated sites along the tubing (generally ± 3 cm from isocenter), the sequence was designed to encode dual pulsatile flow waveforms with high temporal resolution. Acquisition was triggered to begin at the end ''diastolic'' phase of the pulsatile cycle and was typically terminated shortly after the flow peak had passed the downstream measurement site (after 28 echoes or approximately 60 ms in our case). Time-of-flight displacement of each RF-tagged bolus of fluid by motion during the TE intervals (4.6 ms) was recorded as a frequency shift of the acquired echo. Separate off-center fields of view were employed for reading out the upstream and downstream echoes in order to maximize the precision of the observed frequency shift. Using the sequence of Fig. 2a, wave velocities in the thin-wall latex tube were evaluated at a series of ''diastolic'' pressure levels, while maintaining a fixed stroke volume setting (approximately constant pulse pressure) on the pulsatile pump. Roughly the same range of static pressures was investigated as for Fig. 1, in order to allow comparison of these data.

Extracting wave velocities from the MR data typically involved separation of the individual gradient echoes, zero filling of the raw data, Fourier transformation, and measurement of the displacement (in hertz) of the spectral peaks. Plotting peak positions according to their corresponding sequence chronology (i.e., accounting for the variable interpulse intervals of the sequence) resulted in direct replications of the velocity waveforms at each measurement site, as shown in Fig. 3. The ordinate in Fig. 3 can be converted directly to fluid velocity (scale shown on right of figure) by converting the frequency shifts (hertz) to distances (centimeters) and dividing by the echo time. Wave velocities were extracted from such data by dividing the known excitation slice separation (6 cm) by the measured temporal delay between two points corresponding to the half-heights of the rising systolic flow waveforms. That delay is indicated in Fig. 3 by the length of the horizontal line joining the two flow waveforms. These points were determined by fitting a segment of each curve (solid lines in Fig. 3) to a second-order polynomial function and analytically solving for the corresponding time value at the chosen ordinate value. This fitting procedure reduced measurement variability due to inaccuracy of one or two individual data points. Finally, the resulting observed wave velocities were corrected for the instantaneous fluid velocity using Eq. [3]. In Fig. 3, e.g., the correction term v_{fluid} equals 42.3 cm/s.

To provide an independent correlative wavespeed measurement, simultaneous dual pressure traces were recorded with each MR acquisition. Timing marker functions on the oscilloscope were used to assess the temporal delay between the half-heights of the two pressure waveforms, which, in concert with the known transducer separation distance, enabled calculation of the wave propagation rate. Each pressure-based wave velocity result was also corrected for the instantaneous fluid velocity by a factor identical to that applied to the flow-derived data.

Evaluation of pulse pressure (Eq. [4]) was carried out by acquiring similar dynamic MR data from the thick-wall latex tubing, but using a fixed quiescent pressure (40 mm Hg) and varying the stroke volume of the pulsatile pump. In addition to yielding the wavespeed, the MR data (such as shown in Fig. 3) can be interpolated to find the peak fluid velocity directly, which is required for the calculation. Spline fits of the entire flow waveforms were used to estimate the actual peak fluid velocities. For comparison with theory, direct manometric determinations of the pulse pressure were simultaneously performed. The true pulse pressure at magnet isocenter was taken to be the average of the two proximal (upstream and downstream) transducer measurements.

RESULTS

Intraluminal area as a function of pressure for the thin-wall latex tubing is plotted in Fig. 1. Analysis of these data (Eq. [1]) indicates that the distensibility is not constant, but varies with intraluminal pressure. The solid line in the figure represents a third-order polynomial fit to the data points, from which was derived predicted wave velocities (shown in Fig. 4, solid line) over the same pressure interval.

A representative MR-derived pair of velocity waveforms for the thin-wall latex tubing, obtained with a static pressure setting of 50.0 mm Hg is shown in Fig. 3. The temporal offset of the upstream and downstream waveforms due to the finite propagation rate is obvious. From this and other

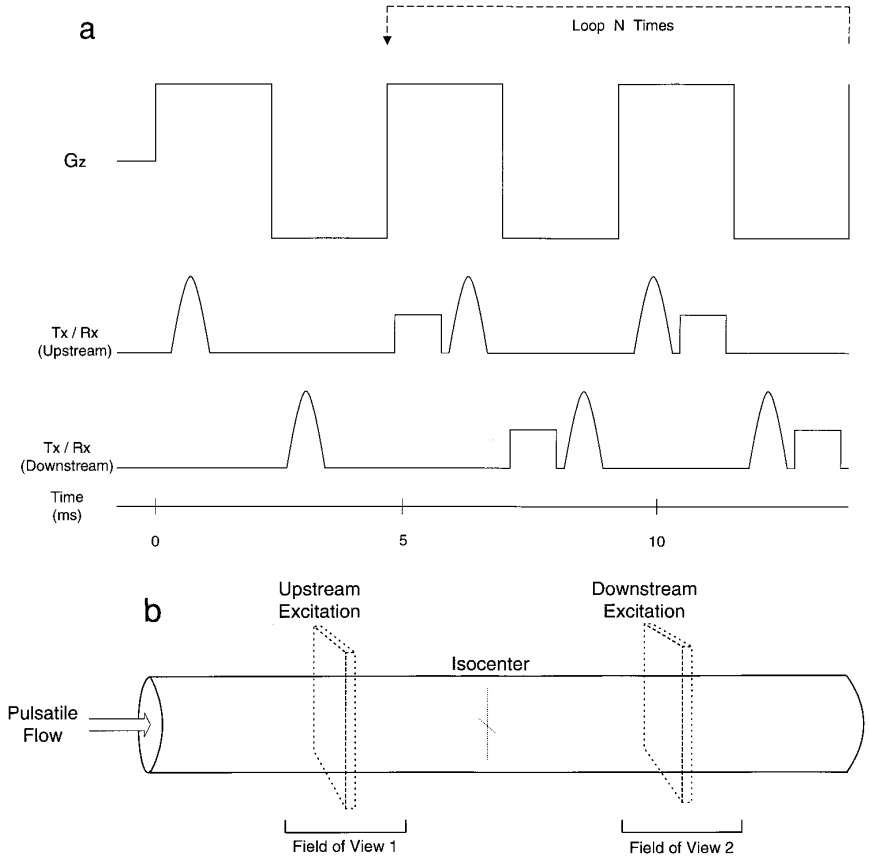

FIG. 2. (a) Timing diagram of the MR sequence used for wave velocity determinations. Gz = gradient along magnet z axis; Tx/Rx = radiofrequency transmission/signal reception, represented by the Gaussian and square waveforms, respectively. Alternating, interleaved RF excitation and signal reception were applied to two (upstream and downstream) sites, which are displayed independently for clarity. Typically, the indicated loop was repeated a total of seven times ($N = 7$) in order to adequately sample the passing systolic flow wave. (b) Sketch of the geometry of the RF excitations and acquisition fields of view with respect to the compliant tubing under study. Excitation slices were generally placed ± 3 cm about isocenter, and each acquisition field of view was 2.56 cm.

similar data, wave velocities were extracted and corrected for fluid velocity as described previously.

Figure 4 presents the pressure-dependent wave velocity results for the thin-wall latex tubing as derived from static distensibility data, dual pressure waveform measurements, and dynamic MR flow wave propagation analyses. As the ''diastolic'' intraluminal pressure increases from 10 to 120 mm Hg, the predicted wave velocity (solid line) is seen to fall from approximately 760 to 530 cm/s. Agreement of the MR flow wave data (solid squares) with that predicted from distensibility measurements (solid line) is particularly good, with a maximum deviation of 5.3%. However, the pressure-derived wave velocities (open circles) are consistently somewhat higher than predicted (5.8–9.5% deviation).

A comparison of pulse pressures in the thick-wall tubing from direct transducer measurements versus those based on Eq. [4] is plotted in Fig. 5. A fixed wave velocity of 15.0 m/s was used in Eq. [4], based on dynamic MR data for this tubing (not shown) obtained at the same ''diastolic'' intraluminal pressure (40 mm Hg). A least-squares fit of the experimental data of Fig. 5 yields the equation $y = 1.014x - 4.72$ (mm Hg), and a correlation coefficient of 0.9997.

DISCUSSION

The projective time-of-flight MR sequence used in this study provides a simple, rapid, and intuitive means to evaluate flow-wave velocities in compliant vessels. Using separate upstream and downstream RF excitation and signal acquisition is less time efficient than a simultaneous multifrequency excitation scheme with a single large field of view (*15*), but is compensated by improved velocity measurement resolution within each smaller field of view. The selected slice separation (6 cm) represents a compromise between the objectives of maximizing the propagation delay while staying well within the homogeneous volume of the B_0 and B_1 magnetic fields. For the range of experimental conditions employed in this study, the total displacement of all RF-tagged spins was less than 6 cm during MR acquisition, thereby

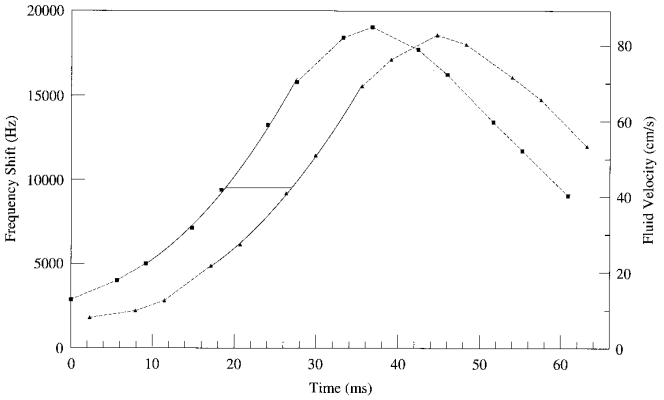

FIG. 3. Systolic flow waveforms for the thin-wall latex tubing as determined using the MR sequence of Fig. 2a. The measured absolute frequency shifts in hertz (left ordinate axis) may be interpreted directly in terms of fluid velocity (right ordinate axis). The propagation delay between the upstream and downstream waveforms was determined at the half-heights (horizontal line) of the pulsatile velocity waveforms.

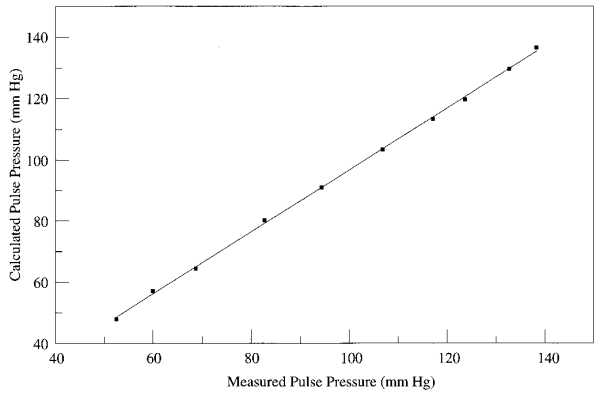

FIG. 5. Correlation of pulse pressures determined manometrically (abscissa) with those calculated using Eq. [4] (ordinate) in the thick-wall ($\frac{3}{4}$ inch i.d.) latex tubing. The linear regression line is $y = 1.014x - 4.72$ (mm Hg); $r = 0.9997$.

avoiding presaturation of downstream spins. For this reason, a relatively large flip angle of 45° was generally used experimentally.

Accurate appraisal of the peak (spatial average) fluid velocity (v_{pk}) is required to solve for the pulse pressure using Eq. [4]. It was observed that the apparent velocity peak of the reconstructed waveforms was increasingly underestimated as the slice separation was increased. For example, peak fluid velocities measured at ±3 cm about isocenter were consistently about 1% lower than those determined at zero offset. For this reason, once the wave velocity was known, the v_{pk} data were acquired using only isocenter excitation and readout (which also effectively doubled the temporal resolution of the data). The accuracy of such a one-dimensional time-of-flight velocity determination also relies on the fluid velocity profile being fairly flat (plug-like), a requirement normally satisfied by strongly accelerated fluid.

The principal limitation of this MR sequence, which is predicated on measurements of the physical displacement of RF-tagged nuclei, is its relatively poor characterization of slow flow. The practical consequence of this is that the onset of systolic flow may not be reliably quantitated, thus obscuring precise identification of the ''foot'' of the flow waveform. This drawback is mainly a result of RF saturation of stationary fluid and the superposition of refocused echoes. Echo refocusing occurs due to the symmetry of the gradient waveform, and in addition to the primary echo (TE 4.6 ms), produces signals with effective times-of-flight of 13.8, 23.0, 32.2, . . . ms. Although at moderate to high velocities, the displaced peaks produced by such higher-order echoes are well separated from the peak of interest, or are outside the field of view, peak overlap at low fluid velocities can cause ambiguities. Accordingly, analysis of the time intervals separating pairs of experimental velocity waveforms (Fig. 3) was consistently performed at the half-heights of the systolic impulses rather than at the foot, a practice that has been validated previously *in vivo* (*16*). The same methodology was also applied for extracting wave velocities from dual pressure waveforms, again due to the uncertain identity of the foot of the systolic upstroke. The ambiguity was doubtless exacerbated by our experimental necessity of keeping the pulsatile pump a certain minimum distance from the magnet and the nonzero compliance of the interposed tubing, which dampened somewhat the otherwise sharp onset of systole at the center of the magnet.

Although the simple MR sequence used in this work cannot be used for *in vivo* work directly, modifications involving presaturation of static tissue surrounding a vessel may be practical. Such a scheme would not reduce the temporal resolution of the actual data-acquisition portion of the se-

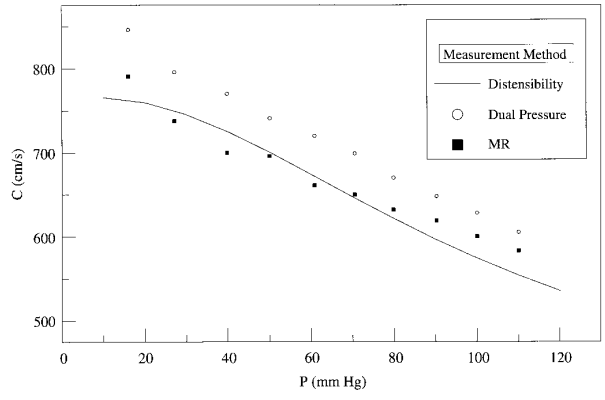

FIG. 4. Compiled wave velocity data as a function of intraluminal pressure for the thin-wall latex tubing. The predicted wave velocity from static distensibility data (solid line) is compared with results of dynamic measurements using MR (closed squares) and dual pressure transducers (open circles).

quence, which is critical to achieving precise wave velocity determinations.

The choice of the $\frac{1}{2}$ inch i.d. thin-wall latex tubing as an experimental model was largely based on the similarity of its wave velocity to that reported for the normal human thoracic and abdominal aorta (*17*). The data of Figs. 1 and 4, however, indicate that the tubing distensibility increased (hence predicted wave velocity decreased) as a function of pressure. In this regard, the tubing behaves unlike arteries, which exhibit decreased compliance at their elastic limits due to their layered, heterogeneous structure (*18*). In addition, the distensibility of arteries is known to vary as a function of anatomic location, falling significantly from the elastic aortic root to the muscular peripheral vessels (*19*). The $\frac{3}{4}$ inch i.d. thick-wall tubing, on the other hand, exhibited distensibility (hence wave velocity) characteristics more representative of the high end of the *in vivo* range. Based on luminal area vs pressure data for this tubing (not shown), the wave velocity is predicted to vary only slightly with intraluminal pressure in the thick-wall tubing. Therefore, little if any change in wave velocity is expected *during* transient pressure impulses, which would otherwise complicate the application of Eq. [4].

The agreement of the MR wave velocities with those predicted from the dependence of luminal area on pressure (Fig. 4) is remarkably good. It should be noted that when the compliant tubing was unconstrained (i.e., supported by a flat, low-friction surface), resulting dynamically measured wave velocities were significantly lower (by about 20%), an observation supported qualitatively by theory (*20*). The dual-pressure-wave propagation data, however, appear to consistently overestimate the predicted values. Several conceivable reasons for this discrepancy come to mind. One potential factor is a small disparity in the temporal response of the two pressure transducers, which would contribute a systematic error to the measurements. Another possible explanation is that it may be inappropriate to correct the pressure-derived wave velocities (Eq. [3]) using the ($v_{pk}/2$) fluid velocity. As noted already, the same correction factors were applied to both the flow- and pressure-derived wave velocities. However, since it is known that the flow waveform is a product of the pressure gradient, and not the pressure *per se*, at the half-height of the pressure waveform, the flow will not also be at one-half of its peak level, but will rather be near or at its peak (*21*). Consequently, the appropriate correction to the observed pressure wave velocity may involve the subtraction of a larger fluid velocity term, which would reduce or possibly eliminate the observed measurement discrepancy. Although using the foot of the pressure waveforms would have in theory abrogated the necessity of a correction, in practice the difficulty of reproducibly identifying such a point would have introduced far greater measurement uncertainty.

The data of Fig. 5 lend credibility to the water-hammer expression (Eq. [4]). The discrepancy between the linear-least-squares fit to the data and the ideal line of identity (4%) is within the achievable accuracy of the wave velocity determination. Alternatively, the peak (spatial average) fluid velocity may have been slightly underestimated by the MR method. The validity of Eq. [4] relies on the assumption that the observed systolic peak of the flow waveform is not influenced by wave reflections, since it is known that reflected pressure waves augment the peak pressure, but reflected flow waves attenuate forward flow (*2*). The effects of reflections in our experiments were minimized by ensuring that no impedance discontinuities existed within a reasonable length of tubing on either side of the magnet center. Thus, reflections generated by tubing couplings (impedance mismatches) did not appear within the test section until after passage of the systolic flow peak. In addition, the rate of pump pulsation was always sufficiently low to allow reflections to dissipate before the next cycle. In the *in vivo* situation, reflective contamination of the aortic systolic peak may also be minimal in persons with healthy, compliant arteries because slower propagation rates in both the forward and reverse directions effectively delays reflected pressure waves until after systole (*22*). Conversely, for individuals with less distensible vessels, accelerated return of reflected waves may alter the apparent systolic pressure amplitude and thereby invalidate pulse pressure measurement using Eq. [4].

CONCLUSIONS

The efficacy of a rapid MR technique for assessing flow-wave velocities in compliant tubes within a single pulsatile cycle has been demonstrated. Agreement of MR wave velocity measurements with those derived via independent means was found to be acceptable (within 10%). Very good agreement was also found between manometrically determined pulse pressures and those calculated from MR data. It is anticipated that similar methods may be profitably applied to quickly and noninvasively investigate arterial compliance and central pulse pressure *in vivo*.

ACKNOWLEDGMENT

This work was supported by a Grant-in-Aid from the American Heart Association, Virginia Affiliate.

REFERENCES

1. W. R. Milnor, ''Hemodynamics,'' 2nd ed., Williams & Wilkins, Baltimore, 1989.
2. W. K. Laskey and W. G. Kussmaul, *Circulation* **75,** 711 (1987).
3. M. F. O'Rourke, J. V. Blazek, C. L. Morreels, and L. J. Krovetz, *Circ. Res.* **23,** 567 (1968).
4. R. P. Kelly, H. Gibbs, M. F. O'Rourke, J. E. Daley, K. Mang, J. J. Morgan, and A. P. Avolio, *Eur. Heart J.* **11,** 138 (1990).

5. J. S. Wright, J. K. Cruickshank, S. Kontis, C. Dore, and R. G. Gosling, *Clin. Sci.* **78,** 463 (1990).
6. R. P. Kelly, C. S. Hayward, A. P. Avolio, and M. F. O'Rourke, *Circulation* **80,** 1652 (1989).
7. C. J. Hardy, B. D. Bolster, E. R. McVeigh, I. E. T. Iben, and E. A. Zerhouni, *Magn. Reson. Med.* **35,** 814 (1996).
8. M. Bock, L. R. Schad, E. Müller, and W. J. Lorenz, *Magn. Reson. Imaging* **13,** 21 (1995).
9. R. H. Mohiaddin, D. N. Firmin, and D. B. Longmore, *J. Appl. Physiol.* **74,** 492 (1993).
10. C. L. Dumoulin, D. J. Doorly, and C. G. Caro, *Magn. Reson. Med.* **29,** 44 (1993).
11. S. N. Urchuk and D. B. Plewes, Abstracts of the Society of Magnetic Resonance, 2nd Annual Meeting, p. 144, 1994.
12. D. A. McDonald and M. G. Taylor, *Prog. Biophys. Chem.* **9,** 107 (1959).
13. C. G. Caro, T. J. Pedley, R. C. Schroter, and W. A. Seed, ''The Mechanics of the Circulation,'' Oxford Univ. Press, Oxford, 1978.
14. E. Müller, A. Weikl, and E. Reinhardt, Abstracts of the Society of Magnetic Resonance in Medicine, 5th Annual Meeting, p. 82, 1986.
15. K. Kraft, F. Corwin, S. Cothran, and P. Fatouros, Abstracts of the Society of Magnetic Resonance in Medicine, 12th Annual Meeting, p. 147, 1993.
16. D. A. McDonald, *J. Appl. Physiol.* **24,** 73 (1968).
17. R. D. Latham, N. Westerhof, P. Sipkema, B. J. Rubal, P. Reuderink, and J. P. Murgo, *Circulation* **72,** 1257 (1985).
18. W. E. Stehbens, ''Hemodynamics and the Blood Vessel Wall,'' Charles C. Thomas, Springfield, IL, 1979.
19. W. W. Nichols and D. A. McDonald, *Med. Biol. Eng.* **10,** 327 (1972).
20. W. R. Milnor and C. D. Bertram, *Circ. Res.* **43,** 870 (1978).
21. D. A. McDonald, *J. Physiol.* **127,** 533 (1955).
22. W. W. Nichols, M. F. O'Rourke, A. P. Avolio, T. Yaginuma, J. P. Murgo, C. J. Pepine, and C. R. Conti, *Am. J. Cardiol.* **55,** 1179 (1985).